BNL-228424-2025-TECH

EIC-ADD-TN-126

HIGH AVERAGE CURRENT HVDC ELECTRON GUN FOR EIC HADRON COOLING

E. Wang

July 2025

Electron-Ion Collider

Brookhaven National Laboratory

U.S. Department of Energy

USDOE Office of Science (SC), Nuclear Physics (NP)

DISCLAIMER

HIGH AVERAGE CURRENT HVDC ELECTRON GUN FOR EIC HADRON COOLING*

E. Wang†,O. Rahman,J. Skaritka,R. Lambiase, J. Biswas, D. Bruno,
J. C. Brutus, M. Gaowei, P. Inacker,K.P. Mondal, M. Paniccia, K. Pandey
Brookhaven National Lab, Upton, NY - 11973 USA
J. Goldlust, P.Dandridge
Dielectric Sciences, Chelmsford, MA - 01824 USA

Abstract

A critical R&D initiative for the Electron Ion Collider (EIC) involves the design of an electron gun capable of generating a high average current and high-brightness electron beam for the hadron cooler. This is essential to preserve hadron beam quality and achieve the collider's luminosity target of $1 \times 10^{34}\,\mathrm{s}^{-1}\,\mathrm{cm}^{-2}$. For an energy recovery linac (ERL)-based hadron cooler, the gun must deliver a high average current of 98.5 mA, a normalized transverse emittance of less than 2 mm−mrad, and a bunch charge of up to 2.5 nC. This proceeding outlines the high-voltage design of a DC gun operating at 500 kV, with conditioning capability up to 600 kV. The design incorporates several unique features, including the use of inverted ceramic at this voltage level, active cooling for the cathode, and large single-crystal multi-alkali cathodes grown on a silicon carbide substrate. High-brightness electron sources are also pivotal for other advanced applications, such as high-intensity gamma sources, future e^+e^- colliders, and ultra-deep UV sources for the semiconductor industry. Additionally, this paper provides an overview of the hadron cooling approaches planned or proposed for the EIC.

INTRODUCTION

To achieve and sustain the high luminosity target of $1 \times 10^{34}\,\mathrm{s}^{-1}\,\mathrm{cm}^{-2}$, the Electron Ion Collider (EIC) requires advanced hadron cooling capabilities. Two hadron cooling systems are planned for the EIC: a low-energy cooler designed to cool hadrons at the injection energy of 24.5 GeV, and a high-energy cooler intended to maintain luminosity at collision energies of 100 GeV and 275 GeV. Both systems will require high-average-current, high-brightness electron sources, particularly if single-pass linac or energy recovery linac (ERL)-based designs are employed for the hadron cooler. The schematic layout of the EIC, including the electron cooler, is shown in Fig. 1.

Building on the successful tests of the polarized gun R&D at the EIC, we are developing a HVDC gun to serve as the electron source for the hadron cooler. This gun is designed to deliver up to 98.5 mA of average current at voltages exceeding 500 kV. The design incorporates several advanced features, including an inverted feedthrough structure and an upgraded active cathode cooling system using fluorinert (FC72). To achieve high brightness, the gun will utilize novel large-crystal K_2CsSb photocathodes grown on 4H-SiC substrates. The design and analysis of the HVDC gun have been completed, and the construction is currently underway. High-voltage conditioning is targeted for 2025, with beam commissioning anticipated in 2026–2027.

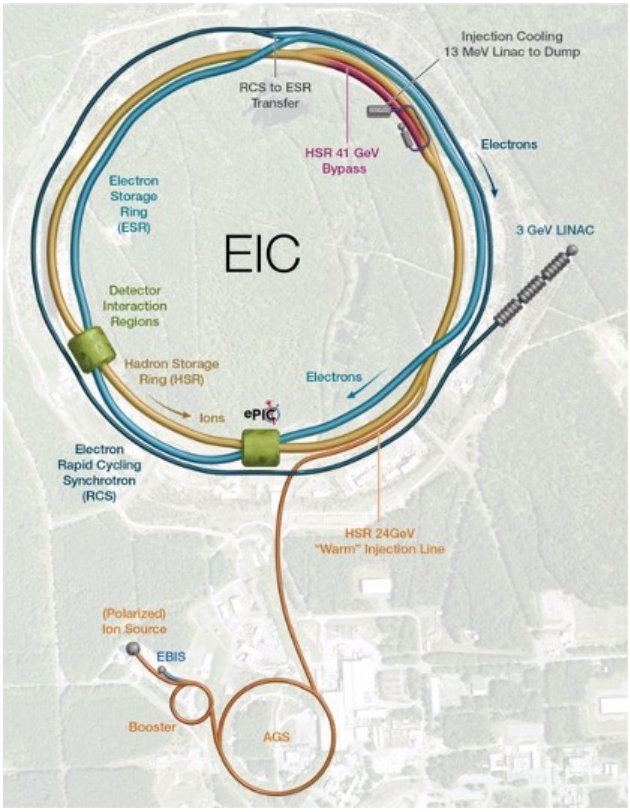

Figure 1: EIC schematic layout.

In this report, we will discuss the ERL-based hadron cooler proposals for the EIC, followed by an overview of the HVDC gun's design concepts, considerations and novel features. Additionally, the major components of the HVDC gun will be described in detail.

VARIOUS PROPOSALS OF THE ERL-BASED HADRON COOLERS FOR EIC

The EIC low-energy cooler (LEC) is designed to reduce the injection rms normalized vertical emittance from

* Work supported by Brookhaven Science Associates, LLC under Contract No. DE-SC0012704 with the U.S. Department of Energy.
† wange@bnl.gov

2 mm mrad to a range of 0.3 mm mrad to 0.5 mm mrad, as reported in [1]. As illustrated in Fig. 2, the design concept is similar to that of the Low-Energy RHIC Electron Cooler (LEReC), includes an increased electron beam energy of 12.5 MeV, a higher beam current of 70 mA, and an extended cooling length of 170 m.

The high-energy cooler (HEC), however, presents more significant challenges. For traditional electron coolers, the cooling rate is inversely proportional to γ^2. To compensate for the reduction in cooling rate at higher energies, several approaches are considered:

- Increasing the six-dimensional phase space density of the electron bunch: Since the electron bunch must match the ion bunch, increasing the bunch charge is a viable strategy. At a repetition rate of 98.5 MHz, the average electron current in the cooling section must exceed 400 mA.
- Extending the cooling section length: Although longer cooling sections improve the cooling rate, they are typically constrained by the available drift space within the hadron ring.
- Pre-cooling the ion bunch: Reducing the transverse velocity spread of ions accelerates the cooling process. The LEC is specifically designed to achieve this pre-cooling.

To mitigate the limitations in cooling rates caused by higher beam energies, stochastic cooling has been developed. This method utilizes a system of pickups, amplifiers, and kickers to cool high-energy hadrons. For even higher cooling rates required for proton cooling, the Coherent Electron Cooler (CeC) has been proposed, leveraging electron plasma as the amplification medium[2, 3].

In recent years, several ERL-based electron cooling systems have been proposed. While storage-based electron cooling systems are also under development, they are not covered in this report as they are not relevant to ERL-based designs.

Strong hadron cooling based on CeC

Strong hadron cooling, as illustrated in Fig. 3a, was adopted in the EIC Conceptual Design Report and has been extensively studied in recent years. The cooling rate is sufficient to balance Intra-beam Scattering (IBS), but achieving precise electron and ion alignment, as well as implementing effective cooling detection, presents substantial challenges. Proposed methods, such as Schottky signal modification, demand detectors with extremely low noise and high gain, which are currently unavailable [4]. Other concerns include the absence of tunable knobs and the difficulty of maintaining a low-noise electron beam in the ERL [5–8]. Generating 1 nC bunch charge with 98.5 mA average current and a cooling section emittance of less than 3 mm mrad requires a high-brightness electron source that surpasses the current state-of-the-art. Consequently, this scheme will necessitate significant R&D efforts[9].

Recirculating ERL-based electron cooling

The average current of 400 mA significantly exceeds the capabilities of demonstrated high-brightness electron sources. To date, the highest average current achieved is approximately 65 mA [10]. To address this limitation, the proposed concept involves using an electron beam to cool the hadron beam over multiple turns before being dumped after energy recovery. By ensuring the beam retains sufficient quality to provide adequate cooling over multiple turns, the average current required from the gun can be reduced proportionally to the number of turns. A harmonic kicker would be employed to remove one bunch and inject another for energy recovery [11]. The schematic illustration in Fig. 3b depicts the original concept developed for JLEIC, which utilized magnetized electron cooling. The electron cooler without using a magnetized beam has been discussed with the EIC team and appears feasible. However, a significant challenge lies in the beam quality degradation caused by multiple turns in the arc section, primarily due to coherent synchrotron radiation (CSR) and the effects of interactions with the high-intensity ion beam using multi-nano Columb high-intensity electron bunches.

Multiple guns beam merging ERL-based electron cooling

To address the limitation of single electron gun average current and mitigate the energy spread increase caused by CSR in multi-turn ERLs, this report proposes an alternative approach to achieve high average current, as illustrated in Fig. 3c. The proposed solution involves a multiple gun merging system. If each gun produces an average current of 100 mA, four guns would be needed to achieve the required 400 mA. Alternatively, using six guns would reduce the average current per gun to 67 mA, a value that has been experimentally demonstrated. The concept of a gun merging system was previously explored during the early EIC conceptual staging. This approach relies on a capacitor kicker to align and stack bunches along a single axis. For instance, to produce a 4 nC, 98.5 MHz beam, each gun would generate 4 nC bunches at a reduced repetition rate of 24.6 MHz. A 24.6 MHz kicker could be implemented using either an LC circuit-based capacitor kicker, as described in [12], or a cavity-based ferrite-dominated RF kicker [13]. After merging, the beam would be accelerated to an energy exceeding 10 MeV for injection into the ERL. This design represents a single-turn ERL system, which is expected to maintain superior beam quality compared to the multi-turn ERL-based electron cooling approach. However, the beam dump power, estimated at 4 MW, exceeds the capacity of typical high-power dumps. To address this, the beam can pass through an RF structure for deceleration. For improved efficiency, an RF output coupling port can be introduced to extract RF power, compensating for the main ERL cavity's power loss resulting from the beam energy recovery process.

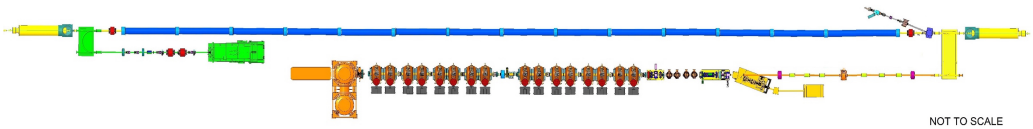

Figure 2: Low-energy cooler layout.

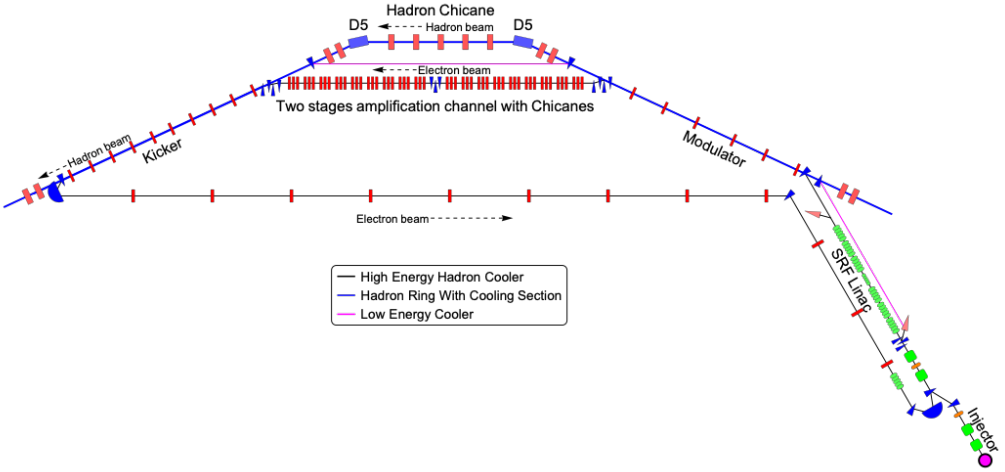

(a) Strong hadron cooling

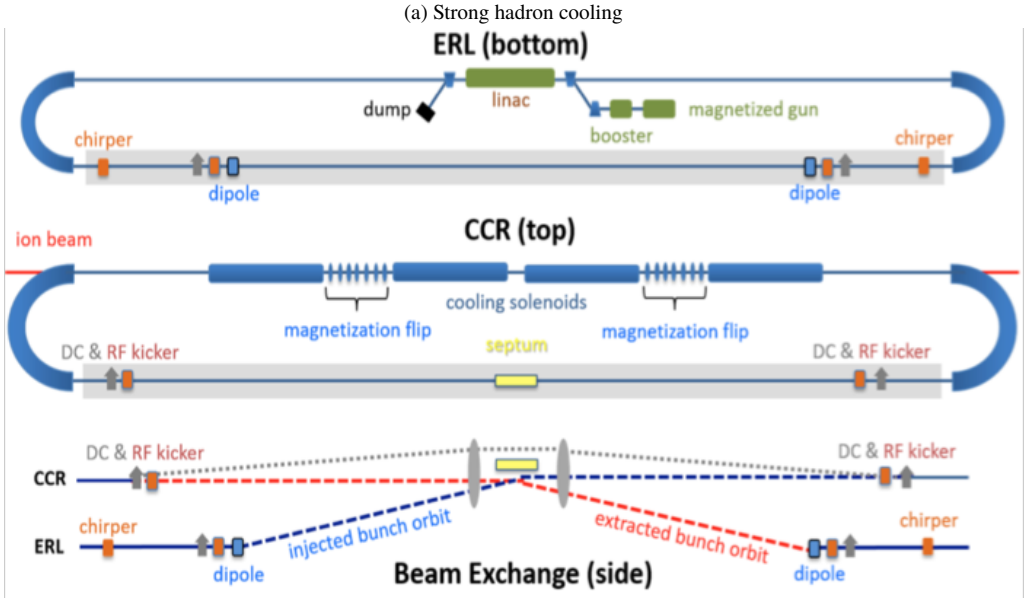

(b) Multi-turn recirculating ERL cooler

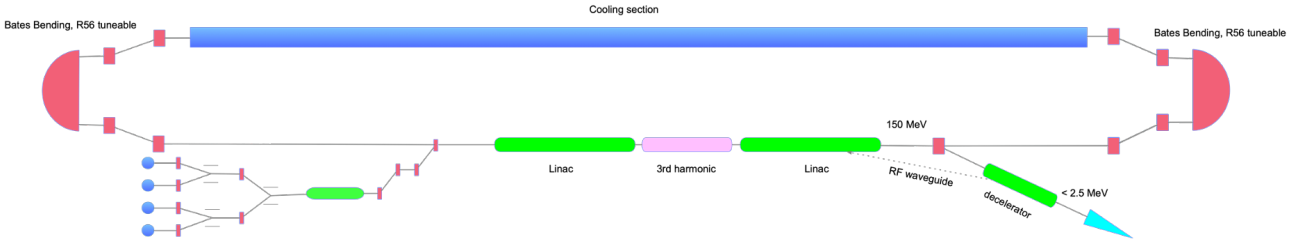

(c) Multi-gun single turn ERL cooler

Figure 3: The schematic drawing of the proposed high energy cooler for EIC

ELECTRON SOURCE DEVELOPMENT

Electron source requirements

All above schemes need high brightness, high average current, high-intensity electron source. We listed the electron source requirements for each scheme as in Table.1. RF guns are generally better suited for generating high-

Table 1: Comparison of different HEC electron source requirements

	Precooler	SHC-CeC	HEC-recirculating	HEC-multi-gun single turn
Average current, mA	>70	90-100 mA	60-100 mA	60-100 mA
Normalized Emittance rms, mm-mrad	1.5	3	2	2
Bunch charge, nC	1.2	1	4	4
Lifetime	1 week	> 3 days	> 3 days	> 3 days

brightness beams with bunch charges above several nC. However, within the EIC timeline, the development of a superconducting radio-frequency (SRF) gun capable of delivering 50 mA to 100 mA is not feasible [14]. Consequently, our approach involves the development of an HVDC gun to generate a pencil-shaped bunch, which is then compressed to the desired length before being injected into the Linac.

The HVDC gun R&D is guided by the following requirements:

- Development of an electron source capable of delivering a 98 mA beam with a single operational lifetime charge of 60 000 C.
- Operation at voltages exceeding 500 kV with an electric field gradient on the cathode surface of more than 5 MV m^{-1}.

The primary challenges of this R&D effort include the development of an efficient cathode cooling mechanism, achieving long stable operation at high voltages, reducing emittance, and generating high-bunch-charge beams [9].

Gun geometry

There are typically two HVDC gun configurations. The first involves placing the high-voltage feedthrough on top of the gun, while the second uses an inverted structure where the feedthrough is located inside the gun body.

The former feedthrough design offers the advantage of better control over the voltage potential along the ceramic, enabling the achievement of high voltages, such as above 500 kV [15]. However, this configuration has significant drawbacks, including a large physical footprint due to the required SF_6 tank and the need to position the high-voltage power supply (HVPS) adjacent to the gun, often sharing the same SF_6 tank. When the gun is placed in a high-radiation environment, such as a collider tunnel, the HVPS inverter is susceptible to radiation damage. Furthermore, challenges remain in developing an efficient cathode cooling system for this setup.

The inverted structure is more compact because both sides of the ceramic are enclosed neither in the atmosphere nor SF_6. This design allows for a shorter ceramic feedthrough. A polarized gun using this configuration has achieved 350 kV after only 20 hours of conditioning[16]. However, scaling this design to higher voltages, such as 500 kV, remains challenging due to uncontrollable potential distributions along the ceramic. We use the triple point shed on both the ground and high voltage sides to linearize the potential along the ceramic as shown in Fig.5 [17]. The sheds also can avoid extremely high gradients at the vacuum-ceramic-metal joint. The inverted structure facilitates cathode cooling and eliminates the need for SF_6 in the entire system. The power supply, located far from high-radiation areas, can be connected to the gun through a high-voltage cable with a plug feedthrough.

A spherical chamber with a spherical electrode provides additional advantages in achieving high voltage. For a given chamber size, the minimum achievable electric field gradient can be optimized by adjusting the electrode size, as shown in Eq. 3:

$$V_{cross} = \int_{R_1}^{R_2} E(r)\, dr = \frac{q}{4\pi\varepsilon_0}\left(R_1^{-1} - R_2^{-1}\right), \quad (1)$$

$$\frac{dE}{dR_1} = 0, \quad (2)$$

$$R_1 = \frac{R_2}{2}. \quad (3)$$

The Pierce-shaped cathode and anode system were optimized to achieve minimal emittance and maximize the laser spot size. Applying 550 kV to the electrode results in a cathode surface gradient of 5.4 MV m^{-1}, while all other surfaces maintain gradients below 10 MV m^{-1}. Even under conditioning up to 600 kV, the maximum surface gradient remains close to 10 MV m^{-1}. With a well-polished surface, field emission can be effectively mitigated. The optimized normalized emittance is 1.02 mm mrad for a bunch length of 250 ps.

To prevent gun trips caused by ion back bombardment, offsetting the laser from the center is essential. A laser offset of 3.5 mm results in approximately 3% emittance degradation. Additionally, 100 ppm HV variation increases emittance by approximately 1%. Emittance will be measured in the beamline using a multi-slit and viewer system. The main geometric design parameters for the gun operating up to 600 kV are summarized in Table 2.

Cathode cooling set up

Characterization of the K_2CsSb cathode material revealed that both the quantum efficiency (QE) and lifetime of the cathode significantly decrease above 80 °C, particularly when the laser power exceeds 5 W, with QE dropping below 1% [18]. Cathode cooling is therefore essential to generate average currents in the 100 mA range, where laser powers typically exceeds 12 W.

We tested a cathode cooling scheme at BNL's polarized gun, which successfully maintained voltages above 300 kV

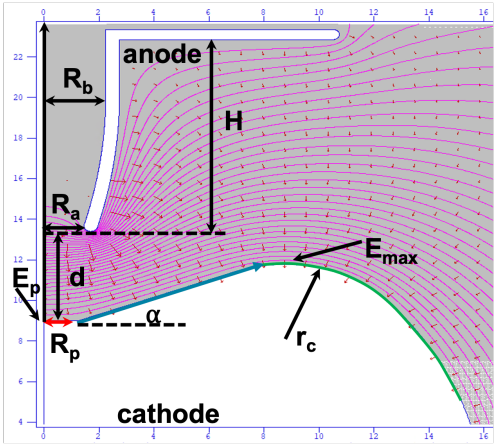

(a) Super fish model of the gun field

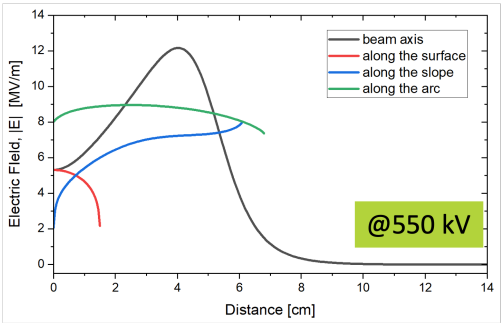

(b) Field gradient along the axis and electrode surface

Figure 4: The HVDC gun field along the various surfaces at 550 kV after optimization

Table 2: Main gun geometry, and field parameters, responding to Fig. 4a

Parameters	Values
R_1 (cm)	16
R_p (cm)	1.26
r_c (cm)	4.8
R_a (cm)	1.45
R_b (cm)	2.25
α (°)	23
d (cm)	4.4
H (cm)	9.5
$E_{cathode}$ (MV m^{-1})	6.4
E_{max} (MV m^{-1})	9.8
Voltage (kV)	600

for over two years without failure[16]. However, the cooling system, using FC72 as a fluid, increased maintenance complexity, as FC72 can dissolve the grease typically used to seal HV cable plugs and feedthroughs. Grease is commonly employed in industry to prevent air from being trapped between these components.

To mitigate the maintenance challenges and enhance cooling efficiency, our new approach involves creating a small gap between the ceramic feedthrough and the HV plug, which is filled with FC72. This not only prevents air entrapment but also provides cooling to the cathode. FC72 has a dielectric strength of 80 kV cm^{-1}, allowing a length of 7.5 cm to withstand 600 kV. This setup is currently under testing, having already achieved voltage levels between 530 and 570 kV. Further tests focusing on stability and reliability are planned.

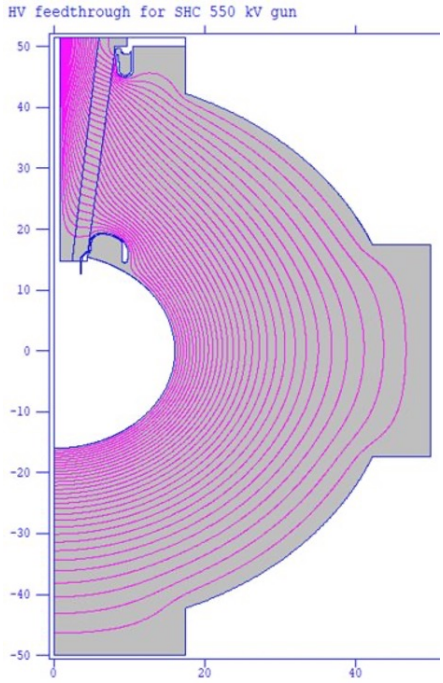

Figure 5: Triple point shielding set up in the gun

The cathode puck, designed with a large-waged base, is tightly attached to the cathode heat sink, which is made of oxygen-free copper. The cooling fluid reaches the heat sink, efficiently removing more than 20 W of thermal power. The cooling setup is still undergoing testing, as illustrated in Fig. 6.

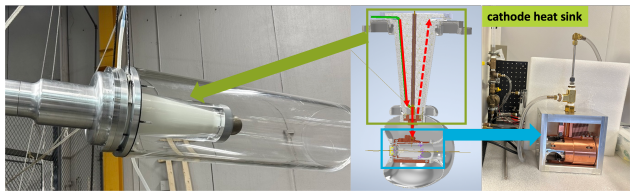

Figure 6: The cathode cooling set up. Left: the high voltage test with the FC72 flowing; Mid: the model shows how the cooling Fluid to the cathode heat sink and returns; Right: The cathode temperature set up using a heater and cooling fluid.

Epitaxially grown large crystal photocathode

When a cathode is deposited onto a metal substrate, it typically forms polycrystalline crystal structures. The used cathode material must then be removed, and the substrate repolished to achieve a mirror-like smoothness. Recently, the BNL team developed a large crystal K_2CsSb cathode,

epitaxially grown on lattice-matched 4H-SiC wafers, which demonstrates exceptional crystal quality, including ultra-smooth surfaces [19, 20]. Using 4H-SiC as the cathode substrate simplifies the replacement process, making it quick, cost-effective, and straightforward.

As discussed in the final section, the 4H-SiC substrate can potentially mitigate high-voltage breakdowns and reduce field emission. Additionally, doped 4H-SiC exhibits excellent thermal conductivity (4.2 W/cm−K), surpassing even copper. This property aids in efficient laser power transfer to the heat sink, helping to maintain the cathode temperature during high current operations. The intrinsic emittance is expected to be smaller than that of the polycrystalline crystal cathodes due to the smoothness of the 4H-SiC surface and the reduced scattering at grain boundaries in the cathode film with ordered crystal structure and large grains. Although the HVDC gun operates at lower gradients, the emittance increase due to surface smoothness may be difficult to measure. However, the reduction of emittance due to reduced grain boundary scattering could potentially be measurable using a slits system. The QE of these photocathodes could reach approximatively 9% when illuminated with a 532 nm laser, which satisfies the operational requirements for the gun. Similar to the cathode puck used in the polarized gun with GaAs wafers, we have designed a similar cathode assembly to accommodate the 4H-SiC wafers.

High voltage cable and HVPS

The gun is designed to operate at 550 kV and is conditioned up to 600 kV. A 1 MV HV cable will be used to deliver the power, which simplifies the configuration compared to the scenario where both the power supply (PS) and the gun share the same SF_6 tank. However, the HVPS and the high-voltage cable's stored energy can potentially damage the gun if arcing occurs. For instance, the HVPS has a stored energy of 3.5 kJ, and a 9-meter 600 kV cable contains 80 J of stored energy. For a 400 kV cable, we have used a semiconductor jacket covering the cable to redistribute energy during discharge [16, 21], though this is not practical for the 1 MV cable. Our new approach involves placing a resistor between the gun and the HV cable.

During conditioning, the field emission current is uncontrollable. To mitigate this, we employ 66.7 MΩ voltage-dividing resistors to form a negative feedback loop, thereby protecting the gun. In high-current operation, the current becomes more controllable. To prevent the resistor from absorbing too much voltage drop, we use a 500 Ω resistor, which provides protection in case of a high-current HV trip. These resistors are capable of handling energies above 4 kJ, which is sufficient for both conditioning and operation of the gun. They are mounted in cylindrical assemblies designed to be directly affixed to the gun assembly. The energy storage between the resistor tank and the gun is negligible.

The HVPS is designed as a two-phase Cockcroft-Walton voltage multiplier, housed within a vessel that can either be pressurized with N_2 or operated with SF_6, depending on the requirements. It can provide an average current of: 1) 150 mA at 400 kV; 2)120 mA at 550 kV; 3) 12 mA at 600 kV.

The voltage multiplier is driven by an external power inverter that operates at a nominal frequency of 20 kHz. The combination of a stored energy of 3.5 kJ and the high-frequency inverter ensures that the output voltage ripple, caused by an instantaneous step of full-load current, remains below 1 kV, as shown in Fig. 7. The voltage drop/ripples due to beam energy variation are on the order of 4×10^{-4}.

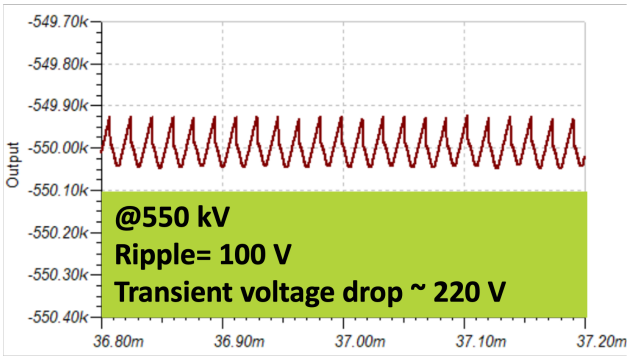

Figure 7: The transient voltage ripple expected at 550 kV operation.

Vacuum

We are aiming to get a similar vacuum level as the polarized gun, about less than 1×10^{-11} torr, to avoid overnight QE degradation. For the R&D beamline which is short, it is important to block the outgassing from the beam dump. Differential pumping stage and beamline with NEG coating were simulated and is going to be used in the SHC R&D gun. Cathode vacuum pressure is $<1 \times 10^{-11}$ Torr when beam dump is at 1×10^{-7} Torr with a full beam power of 55 kW.

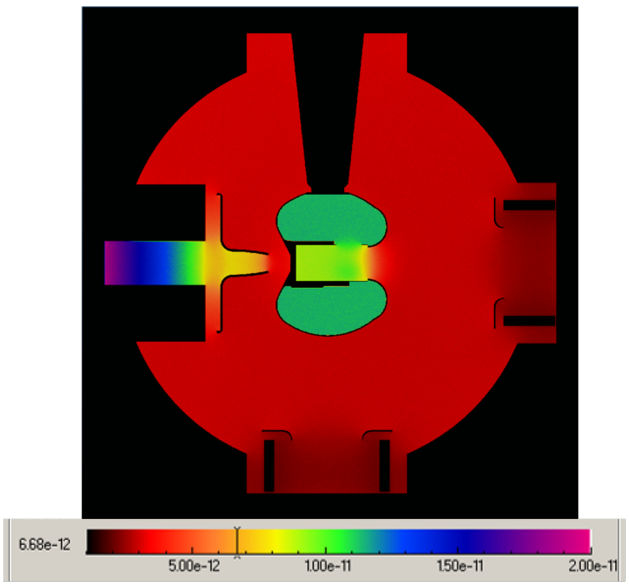

Figure 8: Monte-Carlos simulations shows the residual molecule distribution inside of gun vessel

DISCUSSION: HV TRIP CONSIDERATIONS AND PROPOSED SOLUTIONS

One of the challenges in designing and operating the HVDC electron gun is the occurrence of undesired HV trips that disrupt the gun's operation. Specifically, the HVPS experiences more frequent trips when attempting higher current outputs. The following discussions are summarized detail the tech notes[22].

Several mechanisms have been proposed to explain HVPS trip, including downstream ion origin and cathode emitter bursts causing strong field emission. The ion backbombardment sequence can be characterized as follows: 1) Electron beam ionizes residual downstream gases; 2) Positively charged ions or clusters flow back towards the cathode; 3) High-energy ions (100s keV) halt at the cathode center, fracturing the material and creating an irregular surface; 4) The roughened cathode surface induces field emission, triggering power supply trips. This mechanism explains the increased trip probability with rising average current and damage concentration at the cathode center. Mitigation strategies such as anode biasing which we adopted and ion kicker electrodes have shown limited effectiveness, reducing trip probability only below 10 mA average current. Moreover, ions generated within the HVDC gap remain unaddressed through these methods. A notable contradiction emerges: some cathode damage spots are away from its center, which is the only location that downstream ions can reach.

An alternative explanation involves the formation of sharp surface on the cathode in a high-gradient environment as follows: 1) Fine crystal cathodes exhibit nanoscale roughness or contain transfer-induced particulates; 2) Low electron affinity results in a significantly reduced field emission threshold; 3) High-gradient operation enables field emission or dark current; 4) Field emission further sharpens tips and enhances field intensity; 5) High-power laser-induced localized temperature elevation amplifies field emission; 6) Field emission experiences exponential increase upon surpassing the field enhancement threshold. This mechanism elucidates damage spot occurrence away from the cathode center and increases trip probability at higher current levels. Employing smoother cathodes on atomically smooth substrates can mitigate these effects. Substrate particulate removal through high-pressure rinsing and clean room cathode installation further minimizes potential complications. Both ways will be incorporated into our program.

Despite numerous mitigation attempts, the HVDC gun encounters challenges in achieving 100 mA operation. We propose an additional mechanism wherein electron beam loss on the anode interacts with the monolayer, potentially degassing the anode and generating ions. These ions halt at the cathode, initiating secondary electron emission in a self-reinforcing cycle similar as the multipacting in RF cavities, ultimately potentially tripping the HVPS.

At 100 mA, even a minimal beam loss of 10^{-5} generates 1 μA beam loss. With 550 kV applied, the beam power loss of 0.55 W can induce outgassing or X-ray generation. To reduce the X-ray generation, we utilize titanium (Z=22) as a low-Z anode material at 550 kV DC gap voltage yields approximately 2 mW of X-ray power from lost electrons.

Cathode growth masks constrain cathode size, but growth material vapor diffusion extends beyond the designated area. Laser halo or scattered light can generate electrons from unexpected regions, which, under strong focusing, are prone to anode tube or aperture loss.

Within the DC gun, the initial aperture encountered by the beam is the anode, where electrons can generate hydrogen (H) or hydrogen gas molecules H_2. These ions, commonly trapped in materials or present as a monolayer coating on metal surfaces, are accelerated by the DC electric field, reaching the cathode surface and initiating the generation of secondary electrons. Another mechanism involves X-rays generated from the anode, which can also produce photo electrons. Cathode materials containing alkali metals exhibit a notably high photo yield or high secondary electron yield, often exceeding 100. Consequently, cathode-originating secondary electrons outnumber incident ions and are susceptible to anode loss, further ion generation.

The anode-cathode configuration enables electron-ion oscillation across an expanded area. When secondary yield exceeds unity, multiple iterations cause instantaneous peak current surges, increasing outgassing and ion backbombardment. Ionized gas movement toward the electrode frequently precipitates power supply failure.

Potential mitigation strategies include: 1) Anodizing cathode substrate to limit metal substrate exposure; 2) Employing low secondary yield materials like BN or SiC for cathode substrates or coatings; 3) Optimizing anode geometry to disrupt ion trajectories toward the cathode electrode. The R&D employ the method 2 and 3. And will leave the 1 as the risk mitigation.

CONCLUSION

In this report, we briefly overview the proposed ERL-based high-energy coolers and low-energy coolers for the EIC. All these hadron coolers require a high-average-current, high-brightness electron source. As part of the EIC R&D efforts, we are developing an HVDC gun with a resistor network housed in a pancake container to fully eliminate stored energy.

The gun is designed as a 550 kV inverted structure utilizing a feedthrough with a novel cathode cooling mechanism. Furthermore, a single or large crystalline multialkali photocathode is being implemented. All these efforts are to address the main challenges in high current operation as laser overheating the cathode, as well as minimize high-voltage power supply (HVPS) trips. The project is currently in the construction phase, with high-voltage conditioning planned for mid-2025 and beam commissioning scheduled to begin in 2026.

REFERENCES

[1] A. Fedotov, D. Kayran, and S. Seletskiy, "Accelerator Physics Requirements for Electron Cooler at the EIC Injection Energy," *JACoW*, vol. COOL2023, pp. 1–4, 2024. doi:10.18429/JACoW-COOL2023-MOPAM2R1

[2] V. N. Litvinenko and Y. S. Derbenev, "Coherent electron cooling," *Phys. Rev. Lett.*, vol. 102, p. 114 801, 11 2009. doi:10.1103/PhysRevLett.102.114801

[3] G. Stupakov, "Cooling rate for microbunched electron cooling without amplification," *Phys. Rev. Accel. Beams*, vol. 21, p. 114 402, 11 2018. doi:10.1103/PhysRevAccelBeams.21.114402

[4] W. F. Bergan, M. Blaskiewicz, and G. Stupakov, "Schottky signal modification as a diagnostic tool for coherent electron cooling," *Phys. Rev. Accel. Beams*, vol. 25, p. 094 401, 9 2022. doi:10.1103/PhysRevAccelBeams.25.094401

[5] E. Wang *et al.*, "Electron ion collider strong hadron cooling injector and erl," 2022. doi:10.18429/JACoW-LINAC2022-MO2AA04

[6] E. Wang, J. Qiang, S. Benson, and W. Bergan, "Generating Super-Gaussian distribution and uniform sliced energy spread bunch for EIC strong hadron cooling," *JACoW*, vol. IPAC2024, MOPC23, 2024. doi:10.18429/JACoW-IPAC2024-MOPC23

[7] K. Deitrick *et al.*, "Development of an erl for coherent electron cooling at the electron-ion collider," no. JLAB-ACP-24-4041, 2024. doi:10.18429/JACoW-IPAC2024-THPC40

[8] N. Wang *et al.*, "Optimization of cooling distribution of the eic shc cooler erl," no. JLAB-ACP-24-4074, 2024. doi:10.18429/JACoW-IPAC2024-TUPC43

[9] O. Rahman *et al.*, "High average current DC electron gun for strong hadron cooling," *JACoW*, vol. IPAC2024, WEPC41, 2024. doi:10.18429/JACoW-IPAC2024-WEPC41

[10] J. Maxson, I. Bazarov, B. Dunham, J. Dobbins, X. Liu, and K. Smolenski, "Design, conditioning, and performance of a high voltage, high brightness dc photoelectron gun with variable gap," *Review of Scientific Instruments*, vol. 85, no. 9, p. 093 306, 2014. doi:10.1063/1.4895641

[11] G. T. Park, J. Guo, R. A. Rimmer, H. Wang, and S. Wang, "Beam exchange of a circulator cooler ring with an ultra-fast harmonic kicker," *Phys. Rev. Accel. Beams*, vol. 24, p. 061 002, 6 2021. doi:10.1103/PhysRevAccelBeams.24.061002

[12] E. Wang, "High current polarized electron source for future erhic," *AIP Conference Proceedings*, vol. 1970, no. 1, p. 050 008, 2018. doi:10.1063/1.5040227

[13] I. S. K. Gardner, "Ferrite dominated cavities," in *CERN - Rutherford Accelerator School: RF Engineering for Particle Accelerators*, 1991, pp. 349–374.

[14] E. Wang *et al.*, "Long lifetime of bialkali photocathodes operating in high gradient superconducting radio frequency gun," *Scientific Reports*, vol. 11, no. 1, p. 4477, 2021. doi:10.1038/s41598-021-83997-1

[15] N. Nishimori *et al.*, "Operational experience of a 500 kv photoemission gun," *Phys. Rev. Accel. Beams*, vol. 22, p. 053 402, 5 2019. doi:10.1103/PhysRevAccelBeams.22.053402

[16] E. Wang *et al.*, "High voltage dc gun for high intensity polarized electron source," *Phys. Rev. Accel. Beams*, vol. 25, p. 033 401, 3 2022. doi:10.1103/PhysRevAccelBeams.25.033401

[17] C. Hernandez-Garcia, M. Poelker, and J. Hansknecht, "High voltage studies of inverted-geometry ceramic insulators for a 350 kv dc polarized electron gun," *IEEE Transactions on Dielectrics and Electrical Insulation*, vol. 23, no. 1, pp. 418–427, 2016. doi:10.1109/TDEI.2015.005126

[18] M. Gaowei *et al.*, "High Current Performance of Alkali Antimonide Photocathode in LEReC DC Gun," in *63rd ICFA Advanced Beam Dynamics Workshop on Energy Recovery Linacs*, 2020, WECOXBS02. doi:10.18429/JACoW-ERL2019-WECOXBS02

[19] W. G. Stam *et al.*, "Growth of ultra-flat ultra-thin alkali antimonide photocathode films," *APL Materials*, vol. 12, no. 6, p. 061 114, 2024. doi:10.1063/5.0213461

[20] M. Gaowei *et al.*, "Pulsed laser deposition assisted growth of alkali-based photocathodes," *Proc. IPAC'24*, pp. 2057–2059, doi:10.18429/JACoW-IPAC2024-WEPC42

[21] E. Wang *et al.*, "High-intensity polarized electron gun featuring distributed bragg reflector gaas photocathode," *Applied Physics Letters*, vol. 124, no. 25, p. 254 101, 2024. doi:10.1063/5.0216694

[22] E. Wang, "Particles scattering in a hvdc gun," no. EIC-ADD-TN-082, 2024. doi:10.2172/2281580